

Fig. 2 Genetic analysis of the mutation in *GAMT*. (a) Chromatogram of genomic DNA analysis in a patient shows the heterozygote of c.391G>C (left) and c.578A>G (right). (b) cDNA analysis in the patient shows two aberrantly spliced transcription products (left) and c.578A>G (right). (c) c.391G>C mutation causes two aberrant

splicing products: one with complete exon 3 (64-bp) skipping and the other involving intron 2 insertion (44-bp) followed by exon 3 skipping. (d) Aligned *GAMT* amino acid sequence of the patient with several other animals, revealing Gln193 is highly conserved among species

depleted and clinical symptoms appear. Presymptomatic treatment has been shown to be successful in achieving normal development (Schulze et al. 2006; El-Gharbawy et al. 2013). Even when diagnosed later, creatine supplementation with reduction of GAA by arginine restriction and ornithine supplementation can alleviate symptoms and prevent further progression of the disease (Schulze et al. 2001). *GAMT* deficiency is a good candidate for neonatal mass screening. Elevated GAA levels in neonatal blood (Schulze et al. 2006; El-Gharbawy et al. 2013) and amniotic fluid (Cheillan et al. 2006) have been reported, and validity of these tests needs to be elucidated.

In conclusion, we presented a 38-year-old patient, the first Japanese case of *GAMT* deficiency with two novel gene mutations. We should always include this disorder on the list of differential diagnoses when seeing patients with neurological symptoms such as intellectual disability, epilepsy, behavioral problems, and involuntary movements, since *GAMT* deficiency is a treatable disorder.

Take-Home Message

A 38-year-old patient, the first Japanese case of guanidinoacetate methyltransferase deficiency with two novel gene

mutations (splice site mutation and missense mutation) was reported.

Compliance with Ethics Guidelines

Contributions of Individual Authors

Tomoyuki Akiyama, Hitoshi Osaka, Hiroko Shimbo, and Tomoshi Nakajiri: Drafting/revising the manuscript for content, analysis, and interpretation of data

Katsuhiko Kobayashi, Makio Oka, Fumika Endoh, and Harumi Yoshinaga: Drafting/revising the manuscript for content

Guarantor for the Article

Tomoyuki Akiyama

Details of Funding

None

Details of Ethics Approval

This study was approved by the ethics board at Kanagawa Children's Medical Center.

Conflict of Interest

Tomoyuki Akiyama, Hitoshi Osaka, Hiroko Shimbo, Tomoshi Nakajiri, Katsuhiko Kobayashi, Makio Oka, Fumika Endoh, and Harumi Yoshinaga declare that they have no conflict of interest.

Informed Consent

All procedures followed were in accordance with the ethical standards of the responsible committee on human experimentation (institutional and national) and with the Helsinki Declaration of 1975, as revised in 2000 (5). Informed consent was obtained from all patients for being included in the study.

References

Almeida LS, Verhoeven NM, Roos B et al (2004) Creatine and guanidinoacetate: diagnostic markers for inborn errors in creatine biosynthesis and transport. *Mol Genet Metab* 82:214–219

- Caldeira Araújo H, Smit W, Verhoeven NM et al (2005) Guanidinoacetate methyltransferase deficiency identified in adults and a child with mental retardation. *Am J Med Genet A* 133A: 122–127
- Cheillan D, Salomons GS, Acquaviva C et al (2006) Prenatal diagnosis of guanidinoacetate methyltransferase deficiency: increased guanidinoacetate concentrations in amniotic fluid. *Clin Chem* 52:775–777
- El-Gharbawy AH, Goldstein JL, Millington DS et al. (2013) Elevation of guanidinoacetate in newborn dried blood spots and impact of early treatment in GAMT deficiency. *Mol Genet Metab* (in press)
- Enjoji M, Yanai N (1961) Analytic test for development in infancy and childhood. *Pediatr Int* 4:2–6
- Komoto J, Huang Y, Takata Y et al (2002) Crystal structure of guanidinoacetate methyltransferase from rat liver: a model structure of protein arginine methyltransferase. *J Mol Biol* 320: 223–235
- Leuzzi V, Mastrangelo M, Battini R, Cioni G (2013) Inborn errors of creatine metabolism and epilepsy. *Epilepsia* 54:217–227
- Longo N, Ardon O, Vanzo R et al (2011) Disorders of creatine transport and metabolism. *Am J Med Genet C Semin Med Genet* 157:72–78
- Mercimek-Mahmutoglu S, Stoeckler-Ipsiroglu S, Adami A et al (2006) GAMT deficiency: features, treatment, and outcome in an inborn error of creatine synthesis. *Neurology* 67:480–484
- Salomons GS, van Dooren SJ, Verhoeven NM et al (2003) X-linked creatine transporter defect: an overview. *J Inher Metab Dis* 26: 309–318
- Schulze A, Ebinger F, Rating D, Mayatepek E (2001) Improving treatment of guanidinoacetate methyltransferase deficiency: reduction of guanidinoacetic acid in body fluids by arginine restriction and ornithine supplementation. *Mol Genet Metab* 74:413–419
- Schulze A, Bachert P, Schlemmer H et al (2003) Lack of creatine in muscle and brain in an adult with GAMT deficiency. *Ann Neurol* 53:248–251
- Schulze A, Hoffmann GF, Bachert P et al (2006) Presymptomatic treatment of neonatal guanidinoacetate methyltransferase deficiency. *Neurology* 67:719–721
- Stöckler S, Holzbach U, Hanefeld F et al (1994) Creatine deficiency in the brain: a new, treatable inborn error of metabolism. *Pediatr Res* 36:409–413
- Stöckler S, Hanefeld F, Frahm J (1996a) Creatine replacement therapy in guanidinoacetate methyltransferase deficiency, a novel inborn error of metabolism. *Lancet* 348:789–790
- Stöckler S, Isbrandt D, Hanefeld F, Schmidt B, von Figura K (1996b) Guanidinoacetate methyltransferase deficiency: the first inborn error of creatine metabolism in man. *Am J Hum Genet* 58: 914–922
- Verhoeven NM, Guerland WS, Struys EA, Bouman AA, van der Knaap MS, Jakobs C (2000) Plasma creatinine assessment in creatine deficiency: a diagnostic pitfall. *J Inher Metab Dis* 23: 835–840
- Verhoeven NM, Salomons GS, Jakobs C (2005) Laboratory diagnosis of defects of creatine biosynthesis and transport. *Clin Chim Acta* 361:1–9
- Wada T, Shimbo H, Osaka H (2012) A simple screening method using ion chromatography for the diagnosis of cerebral creatine deficiency syndromes. *Amino Acids* 43:993–997



Contents lists available at ScienceDirect
**Molecular Genetics and
Metabolism Reports**

journal homepage: <http://www.journals.elsevier.com/molecular-genetics-and-metabolism-reports/>



A rapid screening with direct sequencing from blood samples for the diagnosis of Leigh syndrome



Hiroko Shimbo^a, Mariko Takagi^a, Mitsuko Okuda^a, Yu Tsuyusaki^a,
Kyoko Takano^a, Mizue Iai^a, Sumimasa Yamashita^a, Kei Murayama^c,
Akira Ohtake^d, Yu-ichi Goto^e, Noriko Aida^b, Hitoshi Osaka^{a,f,*}

^a Division of Neurology, Kanagawa Children's Medical Center, 2-138-4 Mutsukawa, Minami-ku, Yokohama, Kanagawa 232-8555, Japan

^b Division of Radiology, Kanagawa Children's Medical Center, 2-138-4 Mutsukawa, Minami-ku, Yokohama, Kanagawa 232-8555, Japan

^c Department of Metabolism, Chiba Children's Hospital, 579-1, Heta-cho, Midori-ku, Chiba-shi, Chiba 266-0007, Japan

^d Department of Pediatrics, Faculty of Medicine, Saitama Medical University, 38 Morohongo, Moroyama, Iruma-gun, Saitama 350-0495, Japan

^e Department of Mental Retardation and Birth Defect Research, National Institute of Neuroscience, National Center of Neurology and Psychiatry, 4-1-1 Ogawahigashi-machi, Kodaira-shi, Tokyo 187-8551, Japan

^f Department of Pediatrics, Jichi Medical School, 3311-1 Yakushiji, Shimotsuke-shi, Tochigi 329-0498, Japan

ARTICLE INFO

Article history:

Received 12 February 2014

Accepted 12 February 2014

Available online xxxx

Keywords:

Leigh syndrome
Complex I deficiency
Heteroplasmy
mtDNA mutation

ABSTRACT

Large numbers of genes are responsible for Leigh syndrome (LS), making genetic confirmation of LS difficult. We screened our patients with LS using a limited set of 21 primers encompassing the frequently reported gene for the respiratory chain complexes I (ND1–ND6, and ND4L), IV(SURF1), and V(ATP6) and the pyruvate dehydrogenase E1 α -subunit. Of 18 LS patients, we identified mutations in 11 patients, including 7 in mtDNA (two with ATP6), 4 in nuclear (three with SURF1). Overall, we identified mutations in 61% of LS patients (11/18 individuals) in this cohort. Sanger sequencing with our limited set of primers allowed us a rapid genetic confirmation of more than half of the LS patients and it appears to be efficient as a primary genetic screening in this cohort.

© 2014 The Authors. Published by Elsevier Inc. This is an open access article under the CC BY-NC-ND license (<http://creativecommons.org/licenses/by-nc-nd/3.0/>).

1. Introduction

Leigh syndrome (LS) (OMIM 256000) is an early onset, devastating neurodegenerative disease of the central nervous system (CNS) characterized by symmetrical necrotic lesions in the brainstem, basal

* Corresponding author at: Dept. of Pediatrics, Jichi Medical School, 3311-1 Yakushiji, Shimotsuke-shi, Tochigi 329-0498, Japan. Fax: +81 285 44 6123.

E-mail address: hosaka@jichi.ac.jp (H. Osaka).

<http://dx.doi.org/10.1016/j.ymgmr.2014.02.006>

2214-4269/© 2014 The Authors. Published by Elsevier Inc. This is an open access article under the CC BY-NC-ND license (<http://creativecommons.org/licenses/by-nc-nd/3.0/>).

ganglia and thalamus [1,2]. The symptoms of LS include psychomotor retardation, respiratory difficulties, nystagmus, hypotonia, seizures, myoclonus, ataxia, dystonia, ptosis, ophthalmoplegia and high lactate levels in the blood and cerebrospinal fluid. Mutations in both mitochondrial DNA (mDNA) and nuclear DNA cause LS [3].

LS arises from a deficiency in the enzymes relating to energy production in the mitochondria, such as the respiratory chain complexes I–V, and the pyruvate dehydrogenase complex. Among the enzymes, isolated complex I deficiency is the most frequent oxidative phosphorylation (OXPHOS) defect in children with LS [4,5], followed by a deficiency of complex IV (cytochrome C oxidase) and complex V (ATP synthase). Complex I is composed of seven mDNA encoded NADH dehydrogenase (ND) subunits (ND1–6, ND4L) and at least 38 nuclear DNA subunits [4]. An isolated generalized defect of complex IV is the second most common biochemical abnormalities found in patients with Leigh syndrome [6,7]. *SURF1* mutations, which encode the putative assembly protein of complex IV, have been repeatedly reported [6].

Since a large number of genes are reportedly related to LS, molecular diagnosis appears challenging. However, emerging drugs for LS demand prompt diagnostic confirmation of LS. Although exome sequencing is a powerful method of suspected mitochondrial disorders, it is time and cost consuming, and impractical to be applied to all patients with LS. Based on the reported mutation information, we designed a small set of 21 primers that cover the gene in which LS mutations have been frequently reported [3]. In this study, we have examined the efficacy of our Sanger sequencing method as a genetic screening for LS in 18 unrelated LS cases from one children's hospital. We identified 7 patients with point mutations in mDNA including 2 cases in the *ATP6* gene and five in the *ND* genes. We also elucidated 4 mutations in the nuclear encoded gene, including 3 patients with a mutation in *SURF1* and 1 patient with a mutation in *PDHA1* (pyruvate dehydrogenase E1 α -subunit). Our data suggest that Sanger screening using limited sets of primers is useful as first line screening for LS.

2. Methods

We identified 18 patients from 16 families that met the criteria of LS at our institution (2005–2012). Diagnoses of LS were defined as presenting progressive neurologic disease with signs and symptoms of brain stem and/or basal ganglia abnormalities revealed on MR images. The clinical courses are summarized in Table 1 and Supplementary text. We have designed primers encoding mitochondrial derived subunits for complex I (*ND1-6*, *ND4L*) [3]. Primers were also designed on frequently reported gene *SURF1* from complex IV [7] and *ATP synthase* from complex V [8]. If the blood lactate/pyruvate ratio is less than 10, we first sequenced the *PDHA1* gene (Suppl. Fig. 1) [8]. Methods of genetic analysis, enzyme assays and determination of heteroplasmic rate and associated references are available in the online version of the paper (Suppl. Table 1, Suppl. Table 2, Suppl. text).

3. Results (Table 1, Suppl. Fig. 2)

Of 18 LS patients, we identified gene mutations in 11 patients from 11 families (Table 1, Suppl. Fig. 2). mDNA mutations were identified in 7 patients. An *ND1* mutation of complex I (m3697G>A, p.Gly131Ser) was identified in 2 individuals with homoplasmy. Mutations in *ND3* (m10158T>C, p.Ser34Pro; mutant rate 90% in white blood cell), *ND5* (m13513G>A, p.Asp393Asn; mutant rate 50% in white blood cell) and *ND6* (m14459G>A, p.Ala71Val, homoplasmic state) were identified in a single patient, respectively. One severe patient died at 1 year, and carried a mutation in *ATP6* (m8993T>G, p.Leu156Arg) of complex V of OXPHOS as a homoplasmic state. Instead of T>G, T>C mutation of the same nucleotide, m8993T>C p.Leu156Pro, was observed with homoplasmy in a milder case.

Four patients were identified with mutations in nuclear DNA. *SURF1* mutations were identified in 3 cases, including 2 cases that were compound heterozygous (c.49+1G>T/c.752_753delAG) and (c.574C>T, p.Arg192Trp and c.743C>A, p.Ala248Asp) and 1 case that was homozygous (c.743C>A, p.Ala248Asp). One male patient was identified with a hemizygous mutation (c.121T>C, p.Cys41Arg) in *PDHA1*. Overall, we identified mutations in 61% of LS patients (11/18 individuals) in this cohort.

4. Discussion

Molecular elucidation of LS at the DNA level is challenging. LS has been associated with a variety of genes in either mitochondrial or nuclear encoded DNA [3]. Surprisingly, we could reveal mutations in 61% of LS patients (11/18 individuals).

We disclosed 7 patients with mDNA mutations. From mitochondrial *ND1*, we identified an m3697G>A mutation in 2 unrelated patients, which has been reported previously in association with mitochondrial myopathy, encephalopathy, lactic acidosis, stroke-like episodes (MELAS) [9] and Leber's hereditary optic neuropathy (LHON) [10]. To our knowledge, this is the first report of the m3697G>A/*ND1* gene mutation causing Leigh syndrome. The heteroplasmy rate is reportedly 80% in patients with MELAS (skeletal muscle) and was 56% with LOHN [9,10]. A high mutation load (100%), found in the blood of Patients 1 and 2 may be associated to severe phenotype in our patients [11]. Low level of m3697G>A mutation (~40%) was found in the blood from an asymptomatic mother of Patient 1 (Suppl. Figs. 3 and 4).

For *ND3*, we found a mutation of m10158T>C with 90% of heteroplasmic rate in one patient showing an early onset and very rapid progress. Severe clinical course and high mutant loads are consistent with reported cases with rapid progression and lethal consequences at early childhood [12]. A mutation of m10158T>C was not detected in the mother of Patient 3 in several tissues examined.

We found one patient with *ND5* mutation, m13513G>A which has been described as causing MELAS, LS or overlapping features of the two syndromes [13–15]. We also found one LS patient with m14459G>A/*ND6* mutation that was reported in patients with LHON, dystonia [16] and LS [17]. So far, the phenotype of these two patients is LS without MELAS, LHON.

We found two patients with *ATPase6* mDNA mutations, m8993T>G and T>C, that are frequently reported in the literature [8]. A patient with a T>G mutation usually exhibits earlier onset and more rapid progression compared to T>C mutation at m8993 that was compatible with our patients (Table 1).

We found 4 patients carrying nuclear encoded gene mutations. *SURF1* deficiency is the most frequent cause of LS with complex IV (cytochrome C oxidase) deficiency [7]. We identified 3 patients with the *SURF1* mutations [18]. Pyruvate dehydrogenase deficiency (PDH) is a common cause of primary congenital lactic acidosis. The biochemical features of PDH deficiency is elevated blood lactate and pyruvate levels with a normal lactate/pyruvate ratio [19]. According to the genetic screening flowchart for Leigh syndrome (Suppl. Fig. 1), we confirmed 1 patient with a hemizygous mutation in the *PDHA1* gene with 7 sets of primers.

Recently, new drugs such as EPI-743 have been shown to improve neurological and neuromuscular symptoms in LS [20,21]. Rapid genetic confirmation of mitochondrial disease may help initiate such treatment early. Next gene sequencing is revealing a wide range of dual mutations both mitochondrial and nuclear gene from patients with mitochondrial disorders [22–24]. However, it is costly and time consuming. Aiming to elucidate genetic basis of LS patients, we screened with our limited set of primers. Surprisingly, it allowed us confirmation for more than half of the patients. Therefore, this method appears to be efficient as a primary genetic screening. Our data also implicates that LS consisted of few "common" causative genes and a large number of "rare" genes. We are now undertaking whole mDNA and exome sequencing for negative cases of this method [22–24]. These data, together with increasing data of mutations, would help us improve our screening method.

Supplementary data to this article can be found online at <http://dx.doi.org/10.1016/j.ymgmr.2014.02.006>.

Conflict of interest statement

We have no conflict of interest to disclose.

Acknowledgments

This work was supported in part by a grant of the Innovative Cell Biology by Innovative Technology (Cell Innovation Program) from the Ministry of Education, Culture, Sports, Science and Technology (MEXT), Japan, by Grants-in-Aid of the Research on Intractable Diseases (Mitochondrial Disorder) from the Ministry of Health, Labour and Welfare of Japan (H23-N-I-016), and by Kawano Masanori Memorial Public Interest Incorporated Foundation for Promotion of Pediatrics (24-12).

Table 1
Genetically determined Leigh syndrome in our institution (2005–2012).

Patient	1	2	3	4	5	6	7	8	9	10	11
Age, gender	7 y, M	10 y, F	9 m, F	7 y, M	11 y, M	1 yt, M	2 y, M	4 y, F	9 y, M	25 yt, M	17 y, M
Type of gene	Mito	Mito	Mito	Mito	Mito	Mito	Mito	Nuclear	Nuclear	Nuclear	Nuclear
Gene	<i>ND1</i>	<i>ND1</i>	<i>ND3</i>	<i>ND5</i>	<i>ND6</i>	<i>ATPase6</i>	<i>ATPase6</i>	<i>SURF1</i>	<i>SURF1</i>	<i>SURF1</i>	<i>PDHA1</i>
Complex	I	I	I	I	I	V	V	IV	IV	IV	IV
Mutations	m3697G>A (p.G131S)	m3697G>A (p.G131S)	m10158T>C (p.S34P)	m13513G>A (p.D393N)	m14459G>A (p.A71V)	m8993T>G (p.L156R)	m8993T>C (p.L156P)	c.49+1G>T	c.743 C> A p.A248D	c.574C>T p.R192 W	c.121T>C p.C41R
	Homo (b)	Homo (b,s,h,n)	Hetero (90%) (b)	Hetero (50%) (b)	Homo (b)	Homo (b)	Homo (b)	c.752–753delAG (b)	c.743C> A p.A248D	c.743C>A p.A248D	
Consanguinity	N	N	N	N	N	N	N	N	Y	N	N
Inheritance	Maternal* hetero:40%	N.A.	De novo	N.A.	N.A.	N.A.	N.A.	Maternal/ paternal	Maternal/ paternal	N.A.	N.A.
Age at onset	3 y 9 m	3 y 0 m	0 y 5 m	1 y 6 m	2 y 0 m	6 m	1 y 0 m	1 y 7 m	1 y 9 m	2 y	1 y 0 m
Initial Symptoms	Hypertonia Walk regre	Ataxic gait Walk regre Tremor	Hypotonia Strabismus	Dev. delay	Fever → lethargy	Dev. delay/ seizure Hypotonia/ nystagmus	Fever → lethargy	Ataxic gait	Ataxic gait	Dev. delay Ataxia	Dev. delay
Status	Walk Normal class	Wheelchair Special class	Tracheo Mech. venti	Walk	Wheelchair Normal class	(Respiratory failure)	No sitting	Tracheo Mech. venti	Tracheo Mech. venti	(Respiratory failure)	Walk Special school
RC enzymes ↓	I, IV (m)	I, III, IV (m)	I (f)	Normal (m/f)	I, III (m)	I, IV (m)	N.A.	N.A.	IV (f)	IV (m)	N.A.
Morphological findings in muscle	No RRF	No RRF	N.A.	No RRF	RRF	N.A.	N.A.	N.A.	N.A.	RRF	N.A.

<i>MRI</i>											
Basal ganglia hyperintensities	Y	Y	Y	Y	Y	Y	Y	Y	Y	Y	Y
Brainstem hyperintensities	N	Y	Y	N	N	N	Y	Y	Y	Y	N
Cerebellar atrophy	N	N	N	Y	N	N	N	N	N	Y	Y
<i>Symptoms</i>											
Dysmorphisms	N	N	N	N	N	N	N	Y	Y	N	N
Developmental delay	N	N	Y	Y	N	N	Y	Y	Y	Y	N
Regression	Y	Y	Y	N	N	Y	Y	Y	Y	Y	N
Feeding problems	N	N	Y	N	N	Y	N	N	N	N	N
Ptosis	N	N	N	N	N	N	N	Y	N	N	N
Ophthalmople	N	N	Y	N	N	N	N	Y	N	Y	N
Pyramidal symptoms	Y	Y	Y	Y	Y	N	N	Y	Y	N	Y
Extrapyramidal symptoms	Y	Y	Y	Y	N	Y	N	Y	Y	N	Y
Dystonia	Y	Y	Y	N	N	N	N	Y	Y	N	Y
Hypotonia	N	N	Y	Y	N	Y	Y	Y	Y	N	Y
Ataxia	Y	Y	Y	Y	N	N	N	Y	Y	Y	Y
Neuropathy	N	N	N	N	N	N	N	Y	Y	Y	Y
Others				WPW syndrome			West syndrome				Nystagmus

y: year, m: month, M: male, F: female, mito: mitochondria, Complex: complex in oxidative phosphorylation, b: blood, s: saliva, h: hair, n: nail, RC: respiratory chain, m: muscle, f: fibroblast, RRF: ragged red fibers, N.A.: not analyzed/not determined, N: no, negative, Y: yes, positive, regre: regression, Dev. delay: Developmental delay, Mech.venti: Mechanically ventilated, Ophthalmople: Ophthalmoplegia, *: asymptomatic.

References

- [1] D. Leigh, Subacute necrotizing encephalomyelopathy in an infant, *J. Neurol. Neurosurg. Psychiatry* 14 (1951) 216–221.
- [2] S. Rahman, R.B. Blok, H.H. Dahl, D.M. Danks, D.M. Kirby, C.W. Chow, J. Christodoulou, D.R. Thorburn, Leigh syndrome: clinical features and biochemical and DNA abnormalities, *Ann. Neurol.* 39 (1996) 343–351.
- [3] J. Finsterer, Leigh and Leigh-like syndrome in children and adults, *Pediatr. Neurol.* 39 (2008) 223–235.
- [4] E. Fassone, S. Rahman, Complex I deficiency: clinical features, biochemistry and molecular genetics, *J. Med. Genet.* 49 (2012) 578–590.
- [5] S. Koene, R.J. Rodenburg, M.S. van der Knaap, M.A. Willemsen, W. Sperl, V. Laugel, E. Ostergaard, M. Tarnopolsky, M.A. Martin, V. Nesbitt, J. Fletcher, S. Edvardson, V. Procaccio, A. Slama, L.P. van den Heuvel, J.A. Smeitink, Natural disease course and genotype–phenotype correlations in complex I deficiency caused by nuclear gene defects: what we learned from 130 cases, *J. Inher. Metab. Dis.* 35 (2012) 737–747.
- [6] Z. Zhu, J. Yao, T. Johns, K. Fu, I. De Bie, C. Macmillan, A.P. Cuthbert, R.F. Newbold, J. Wang, M. Chevrette, G.K. Brown, R.M. Brown, E.A. Shoubridge, SURF1, encoding a factor involved in the biogenesis of cytochrome c oxidase, is mutated in Leigh syndrome, *Nat. Genet.* 20 (1998) 337–343.
- [7] Y. Wedatilake, R. Brown, R. McFarland, J. Yapliito-Lee, A.A. Morris, M. Champion, P.E. Jardine, A. Clarke, D.R. Thorburn, R.W. Taylor, J.M. Land, K. Forrest, A. Dobbie, L. Simmons, E.T. Aasheim, D. Ketteridge, D. Hanrahan, A. Chakrapani, G.K. Brown, S. Rahman, SURF1 deficiency: a multi-centre natural history study, *Orphanet J. Rare Dis.* 8 (2013) 96.
- [8] M. Makino, S. Horai, Y. Goto, I. Nonaka, Mitochondrial DNA mutations in Leigh syndrome and their phylogenetic implications, *J. Hum. Genet.* 45 (2000) 69–75.
- [9] D.M. Kirby, R. McFarland, A. Ohtake, C. Dunning, M.T. Ryan, C. Wilson, D. Ketteridge, D.M. Turnbull, D.R. Thorburn, R.W. Taylor, Mutations of the mitochondrial ND1 gene as a cause of MELAS, *J. Med. Genet.* 41 (2004) 784–789.
- [10] L. Spruijt, H.J. Smeets, A. Hendrickx, M.W. Bettink-Remeijer, A. Maat-Kievit, K.C. Schoonderwoerd, W. Sluiter, I.F. de Co, R.Q. Hintzen, A MELAS-associated ND1 mutation causing leber hereditary optic neuropathy and spastic dystonia, *Arch. Neurol.* 64 (2007) 890–893.
- [11] A.L. Mitchell, J.L. Elson, N. Howell, R.W. Taylor, D.M. Turnbull, Sequence variation in mitochondrial complex I genes: mutation or polymorphism? *J. Med. Genet.* 43 (2006) 175–179.
- [12] R. McFarland, D.M. Kirby, K.J. Fowler, A. Ohtake, M.T. Ryan, D.J. Amor, J.M. Fletcher, J.W. Dixon, F.A. Collins, D.M. Turnbull, R.W. Taylor, D.R. Thorburn, De novo mutations in the mitochondrial ND3 gene as a cause of infantile mitochondrial encephalopathy and complex I deficiency, *Ann. Neurol.* 55 (2004) 58–64.
- [13] A. Sudo, S. Honzawa, I. Nonaka, Y. Goto, Leigh syndrome caused by mitochondrial DNA G13513A mutation: frequency and clinical features in Japan, *J. Hum. Genet.* 49 (2004) 92–96.
- [14] M. Crimi, S. Galbiati, I. Moroni, A. Bordoni, M.P. Perini, E. Lamantea, M. Sciacco, M. Zeviani, I. Biunno, M. Moggio, G. Scarlato, G.P. Comi, A missense mutation in the mitochondrial ND5 gene associated with a Leigh–MELAS overlap syndrome, *Neurology* 60 (2003) 1857–1861.
- [15] A. Brautbar, J. Wang, J.E. Abdenur, R.C. Chang, J.A. Thomas, T.A. Grebe, C. Lim, S.W. Weng, B.H. Graham, L.J. Wong, The mitochondrial 13513G>A mutation is associated with Leigh disease phenotypes independent of complex I deficiency in muscle, *Mol. Genet. Metab.* 94 (2008) 485–490.
- [16] A. Gropman, T.J. Chen, C.L. Perng, D. Krasnewich, E. Chernoff, C. Tiff, L.J. Wong, Variable clinical manifestation of homoplasmic G14459A mitochondrial DNA mutation, *Am. J. Med. Genet. A* 124A (2004) 377–382.
- [17] D.M. Kirby, S.G. Kahler, M.L. Freckmann, D. Reddihough, D.R. Thorburn, Leigh disease caused by the mitochondrial DNA G14459A mutation in unrelated families, *Ann. Neurol.* 48 (2000) 102–104.
- [18] J. Tanigawa, K. Kaneko, M. Honda, H. Harashima, K. Murayama, T. Wada, K. Takano, M. Iai, S. Yamashita, H. Shimbo, N. Aida, A. Ohtake, H. Osaka, Two Japanese patients with Leigh syndrome caused by novel SURF1 mutations, *Brain Dev.* 34 (2012) 861–865.
- [19] L. De Meirleir, Defects of pyruvate metabolism and the Krebs cycle, *J. Child Neurol.* 17 (Suppl. 3) (2002) 3S26–33 (discussion 3S33–24).
- [20] A.A. Sadun, C.F. Chicani, F.N. Ross-Cisneros, P. Barboni, M. Thoolen, W.D. Shrader, K. Kubis, V. Carelli, G. Miller, Effect of EPI-743 on the clinical course of the mitochondrial disease Leber hereditary optic neuropathy, *Arch. Neurol.* 69 (2012) 331–338.
- [21] D. Martinelli, M. Catteruccia, F. Piemonte, A. Pastore, G. Tozzi, C. Dionisi-Vici, G. Pontrelli, T. Corsetti, S. Livadiotti, V. Kheifets, A. Hinman, W.D. Shrader, M. Thoolen, M.B. Klein, E. Bertini, G. Miller, EPI-743 reverses the progression of the pediatric mitochondrial disease—genetically defined Leigh syndrome, *Mol. Genet. Metab.* 107 (2012) 383–388.
- [22] D.S. Lieber, S.E. Calvo, K. Shanahan, N.G. Slate, S. Liu, S.G. Hershman, N.B. Gold, B.A. Chapman, D.R. Thorburn, G.T. Berry, J.D. Schmahmann, M.L. Borowsky, D.M. Mueller, K.B. Sims, V.K. Mootha, Targeted exome sequencing of suspected mitochondrial disorders, *Neurology* 80 (2013) 1762–1770.
- [23] J.T. Dare, V. Vasta, J. Penn, N.T. Tran, S.H. Hahn, Targeted exome sequencing for mitochondrial disorders reveals high genetic heterogeneity, *BMC Med. Genet.* 14 (2013) 118–126.
- [24] D.L. Dinwiddie, L.D. Smith, N.A. Miller, A.M. Atherton, E.G. Farrow, M.E. Strenk, S.E. Soden, C.J. Saunders, S.F. Kingsmore, Diagnosis of mitochondrial disorders by concomitant next-generation sequencing of the exome and mitochondrial genome, *Genomics* 102 (2013) 148–156.

Expanding the phenotypic spectrum of *TUBB4A*-associated hypomyelinating leukoencephalopathies

Satoko Miyatake, MD,
PhD
Hitoshi Osaka, MD, PhD
Masaaki Shiina, MD,
PhD
Masayuki Sasaki, MD,
PhD
Jun-ichi Takanashi, MD,
PhD
Kazuhiro Haginoya, MD,
PhD
Takahito Wada, MD,
PhD
Masafumi Morimoto,
MD, PhD
Naoki Ando, MD, PhD
Yoji Ikuta, MD
Mitsuko Nakashima,
MD, PhD
Yoshinori Tsurusaki, PhD
Noriko Miyake, MD,
PhD
Kazuhiro Ogata, MD,
PhD
Naomichi Matsumoto,
MD, PhD
Hirotomo Saitsu, MD,
PhD

Correspondence to
Dr. Matsumoto:
naomat@yokohama-cu.ac.jp
or Dr. Saitsu:
hsaitsu@yokohama-cu.ac.jp

Supplemental data
at Neurology.org

ABSTRACT

Objective: We performed whole-exome sequencing analysis of patients with genetically unsolved hypomyelinating leukoencephalopathies, identifying 8 patients with *TUBB4A* mutations and allowing the phenotypic spectrum of *TUBB4A* mutations to be investigated.

Methods: Fourteen patients with hypomyelinating leukoencephalopathies, 7 clinically diagnosed with hypomyelination with atrophy of the basal ganglia and cerebellum (H-ABC), and 7 with unclassified hypomyelinating leukoencephalopathy, were analyzed by whole-exome sequencing. The effect of the mutations on microtubule assembly was examined by mapping altered amino acids onto 3-dimensional models of the $\alpha\beta$ -tubulin heterodimer.

Results: Six heterozygous missense mutations in *TUBB4A*, 5 of which are novel, were identified in 8 patients (6/7 patients with H-ABC [the remaining patient is an atypical case] and 2/7 patients with unclassified hypomyelinating leukoencephalopathy). In 4 cases with parental samples available, the mutations occurred de novo. Analysis of 3-dimensional models revealed that the p.Glu410Lys mutation, identified in patients with unclassified hypomyelinating leukoencephalopathy, directly impairs motor protein and/or microtubule-associated protein interactions with microtubules, whereas the other mutations affect longitudinal interactions for maintaining $\alpha\beta$ -tubulin structure, suggesting different mechanisms in tubulin function impairment. In patients with the p.Glu410Lys mutation, basal ganglia atrophy was unobserved or minimal although extrapyramidal features were detected, suggesting its functional impairment.

Conclusions: *TUBB4A* mutations cause typical H-ABC. Furthermore, *TUBB4A* mutations associate cases of unclassified hypomyelinating leukoencephalopathies with morphologically retained but functionally impaired basal ganglia, suggesting that *TUBB4A*-related hypomyelinating leukoencephalopathies encompass a broader clinical spectrum than previously expected. Extrapyramidal findings may be a key for consideration of *TUBB4A* mutations in hypomyelinating leukoencephalopathies. *Neurology*® 2014;82:2230-2237

GLOSSARY

4H = hypomyelination, hypodontia, and hypogonadotropic hypogonadism; **H-ABC** = hypomyelination with atrophy of the basal ganglia and cerebellum; **MAP** = microtubule-associated protein; **MREI** = Met-Arg-Glu-Ile; **TUBB4A** = tubulin, beta 4A class IVa.

Leukoencephalopathies are a heterogeneous group of disorders affecting the white matter of the brain. It is estimated that approximately 30% to 40% of patients with leukoencephalopathy remain without a specific diagnosis despite extensive investigations.¹ Brain MRI aids diagnosis because distinct MRI patterns enable easier detection of white matter abnormalities and successful categorization.^{1,2} Moreover, recent advances in whole-exome sequencing have improved understanding of these clinically defined/undefined disease entities by identifying genetic causes and their phenotypic spectrum. For example, the majority of cases with hypomyelination,

From the Departments of Human Genetics (S.M., M.N., Y.T., N. Miyake, N. Matsumoto, H.S.) and Biochemistry (M. Shiina, K.O.), Yokohama City University Graduate School of Medicine; Division of Neurology (H.O.), Clinical Research Institute, Kanagawa Children's Medical Center, Yokohama; Department of Pediatrics (H.O.), Jichi Medical School, Tochigi; Department of Child Neurology (M. Sasaki), National Center of Neurology and Psychiatry, Tokyo; Department of Pediatrics (J.-i.T.), Kameda Medical Center, Chiba; Department of Pediatric Neurology (K.H.), Takuto Rehabilitation Center for Children, Sendai; Genetic Counselling and Clinical Research Unit (T.W.), Kyoto University School of Public Health; Department of Pediatrics (M.M.), Graduate School of Medical Science, Kyoto Prefectural University of Medicine; Department of Neonatology and Pediatrics (N.A.), Nagoya City University Graduate School of Medical Sciences; and Department of Neurology (Y.I.), Tokyo Metropolitan Children's Medical Center, Japan.

Go to Neurology.org for full disclosures. Funding information and disclosures deemed relevant by the authors, if any, are provided at the end of the article.

hypodontia, and hypogonadotropic hypogonadism (4H syndrome),³⁻⁵ tremor-ataxia with central hypomyelination leukodystrophy (TACH),⁶ leukodystrophy with oligodontia (LO),^{7,8} or hypomyelination with cerebellar atrophy and hypoplasia of the corpus callosum (HCAHC),⁹ which was described in Japan, share some clinical overlap and have *POLR3A* or *POLR3B* mutations in common.¹⁰⁻¹⁴

Hypomyelination with atrophy of the basal ganglia and cerebellum (H-ABC)^{15,16} is characterized by early-onset motor regression and/or delay followed by extrapyramidal symptoms, distinguishing H-ABC from other hypomyelinating leukoencephalopathies caused by *POLR3A* or *POLR3B* mutations. A recurrent de novo *TUBB4A* mutation was recently reported in 11 patients with H-ABC.¹⁷ Of note, *TUBB4A* mutations also cause autosomal dominant *DYT4* dystonia,^{18,19} a condition that presents with normal brain MRI findings. This suggests that in addition to H-ABC, *TUBB4A* mutations may be widely related to other hypomyelinating leukoencephalopathies. Herein, we describe 8 patients with *TUBB4A* mutations identified by whole-exome sequencing, clarifying their phenotypic spectrum.

METHODS Study subjects. Fourteen patients with molecularly undiagnosed hypomyelinating leukoencephalopathy were included in the study. Patients were diagnosed based on clinical symptoms and brain MRI findings. Among the 14 patients, 7 were clinically diagnosed with H-ABC and 7 with hypomyelinating leukoencephalopathy that did not meet the criteria for H-ABC, 4H syndrome, or Pelizaeus-Merzbacher disease. Patients with *POLR3A* or *POLR3B* mutations were excluded from this cohort. When available, parental samples were also tested in mutation-positive patients.

Standard protocol approvals, registrations, and patient consents. Experimental protocols were approved by the Committee for Ethical Issues at Yokohama City University School of Medicine. Written informed consent was obtained from all patients or their parents.

Mutation analysis. We performed whole-exome sequencing in 14 patients. Genomic DNA was captured using the SureSelect^{XT} Human All Exon 50 Mb (v3) or 51 Mb (v4) Kit (Agilent Technologies, Santa Clara, CA) and sequenced on either the GAIIX platform (Illumina, San Diego, CA) with 108-base pair paired-end reads or HiSeq2000 (Illumina) with 101-base pair paired-end reads. After filtering against dbSNP135 and 91 in-house normal control exomes, rare protein-altering and splice-site variant calls were obtained for each patient. We identified *TUBB4A* mutation calls and confirmed these mutations by Sanger sequencing. In 4 of 8 patients with *TUBB4A* mutations, parental samples were analyzed by Sanger sequencing to determine the mode of inheritance.

Three-dimensional structure modeling. To determine the effect of *TUBB4A* mutations on microtubule assembly, we mapped mutation positions onto the 3-dimensional structure of the $\alpha\beta$ -tubulin heterodimer (Protein Data Bank code 1JFF)²⁰ and examined their interaction with surrounding molecules.

RESULTS Identification of *TUBB4A* mutations. Whole-exome sequencing identified 6 heterozygous missense mutations in *TUBB4A*, in 6 of 7 patients with H-ABC (85.7%) and 2 of 7 patients with unclassified hypomyelinating leukoencephalopathy (28.6%) (see table 1 and tables e-1 and e-2 on the *Neurology*[®] Web site at Neurology.org). Two mutations, c.1228G>A (p.Glu410Lys) and c.745G>A (p.Asp249Asn), were identified in 2 unrelated patients. Two hypomyelinating patients with similar clinical features as those previously reported,⁹ carried the c.1228G>A mutation. The c.745G>A mutation was a recurrent mutation reported in patients with H-ABC.¹⁷ The other 5 mutations were novel. None of the mutations were registered in the National Heart, Lung, and Blood Institute Exome Sequencing Project (ESP6500), 1000 Genomes, or our 575 in-house control exomes. The c.5G>A (p.Arg2Gln) missense mutation, identified in a patient with H-ABC, alters Arg2 to Gln. Arg2 is located within the highly conserved, amino-terminal β -tubulin tetrapeptide Met-Arg-Glu-Ile (MREI) motif and is involved in autoregulatory mechanisms for β -tubulin stability. Notably, Arg2 is altered to Gly in a large family with *DYT4*.^{18,19} All of the mutations occur within highly conserved residues, from yeast to human, and among human β -tubulins (figure 1). GERP (Genomic Evolutionary Rate Profiling) scores were high for all mutated residues, and Web-based prediction programs identified all mutations as pathogenic (table e-1). In 4 patients with parental samples available, the mutations occurred de novo (table e-1). In 2 patients, only the mother's sample was available and confirmed as mutation-negative.

Three-dimensional structural modeling analysis. Tubulin heterodimers polymerize longitudinally in a head-to-tail manner, forming protofilaments, which then laterally interact with each other to form microtubules (figure 2). Some mutations fall within longitudinal interaction interfaces, whereas others are near interaction regions for motor proteins and microtubule-associated proteins (MAPs).^{21,22} Thr178 of β -tubulin is located at a longitudinal interheterodimer interface, in proximity to the guanine nucleotide-binding pocket of β -tubulin (figure 2). This residue is reportedly important for regulation of $\alpha\beta$ -tubulin heterodimer polymerization with GTP^{23,24}; therefore, the Thr178Arg mutation may affect the polymerization process. Arg2 and Asp249 of β -tubulin are

Table 1 Clinical features of the patients

	Patient 1 ^a	Patient 2 ^a	Patient 3	Patient 4 ²⁶	Patient 5 ²⁷	Patient 6	Patient 7	Patient 8
Current age, y, sex	23, M	41, M	15, F	12, M	16, M	10, M	4, M	1, F
Mutation	c.1228G>A	c.1228G>A	c.5G>A	c.745G>A	c.1162A>G	c.745G>A	c.533C>G	c.785G>A
Protein alteration	p.Glu410Lys	p.Glu410Lys	p.Arg2Gln	p.Asp249Asn	p.Met388Val	p.Asp249Asn	p.Thr178Arg	p.Arg262His
Initial diagnosis	Unclassified hypomyelinating leukoencephalopathy ^a	Unclassified hypomyelinating leukoencephalopathy ^a	H-ABC	H-ABC	H-ABC	H-ABC	H-ABC	H-ABC
Age at onset, mo	12	12	1.5	18	3	19	6	2
Maximum motor milestone	Unsupported unstable walking	Unsupported unstable walking	No head control	Walking for a few steps	Rolling over	Supported walking	No head control	No head control
Onset of motor deterioration	10 y	20 y	ND	18 mo	3 mo	19 mo	ND	ND
Intellectual disability	Mild	Moderate	Severe	Severe	Severe	Severe	Severe	Moderate
Motor signs								
Ataxia	+	+	ND	+	ND	+	ND	ND
Tremor	+	+	-	-	-	+	-	ND
Spasticity	+	+	+	+	+	+	ND	+
Babinski sign	+	+	-	+	ND	+	-	+
Rigidity	+	+	+	+	+	+	+	-
Choreoathetosis	-	-	+	+	+	-	-	-
Dystonia	+	+	+	+	+	+	-	-
Brain MRI findings								
Hypomyelination	+	+	+	+	+	+	+	+
Atrophy of the basal ganglia	-	±	+	+	+	+	+	+
Atrophy of the cerebellum	+	+	+	+	+	+	+	-
Atrophy of the corpus callosum	+	+	+	+	+	+	+	-

Abbreviations: H-ABC = hypomyelination with atrophy of the basal ganglia and cerebellum; ND = not determined.

Symbols: + = present; - = absent; ± = minimally detected.

^aUnclassified hypomyelinating leukoencephalopathy: did not meet the criteria for H-ABC, 4H syndrome (hypomyelination, hypodontia, and hypogonadotropic hypogonadism), or Pelizaeus-Merzbacher disease.

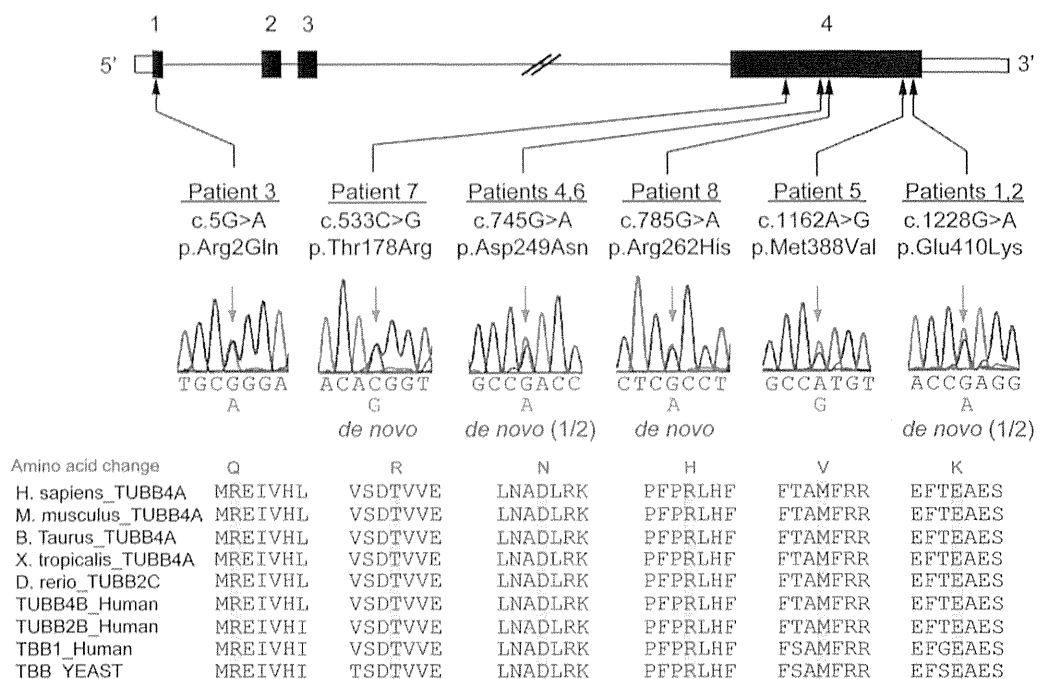
located at an intraheterodimer interface (figures 2 and e-1A). These residues stabilize the β -tubulin T7 loop region, which interacts with α -tubulin within a heterodimer (figure e-1A), indicating that the p.Arg2Gln and p.Asp249Asn mutations may affect tubulin heterodimerization. Glu410 is located on the exposed outer surface that mediates interactions with motor proteins and/or MAPs (figures 2 and e-1B).^{21,22} This residue is crucial for the kinesin-microtubule interaction, and thus the p.Glu410Lys mutation may directly impair motor protein and/or MAP interactions with microtubules. Arg262 and Met388 are located near the intra- and interheterodimer interfaces, respectively, and both are also near the interaction region for motor proteins and/or MAPs (figures 2 and e-1, B and C). Arg262 is involved in the hydrophobic core with residues from a loop that interacts with the α -tubulin subunit within the heterodimer, and from helix H12,

which interacts with motor proteins and/or MAPs (figures 2 and e-1B). Met388 is involved in the hydrophobic core with residues from helix H11, which interacts with the α -tubulin subunit in the neighboring heterodimer, and from helix H12 (figures 2 and e-1C).²⁵ Thus, the p.Arg262His and the p.Met388Val mutations may destabilize the hydrophobic core and potentially affect the tertiary structure, resulting in impairment of longitudinal intra- and interheterodimer tubulin interactions, respectively, and/or interaction with motor proteins and/or MAPs.

Clinical features. Clinical information on patients with *TUBB4A* mutations is presented in tables 1 and e-2, and brain MRIs are shown in figures 3 and e-2.

The mean age at onset was 9.2 months, although the age at onset was varied. Initial motor development also varied, with some acquiring unsupported but

Figure 1 *TUBB4A* mutations in patients with hypomyelinating leukoencephalopathy



TUBB4A schematic with the 6 mutations is presented. Untranslated regions and coding regions are shown in white and black rectangles, respectively. All mutations occur at evolutionarily conserved amino acids. Homologous sequences were aligned using CLUSTALW (<http://www.genome.jp/tools/clustalw/>).

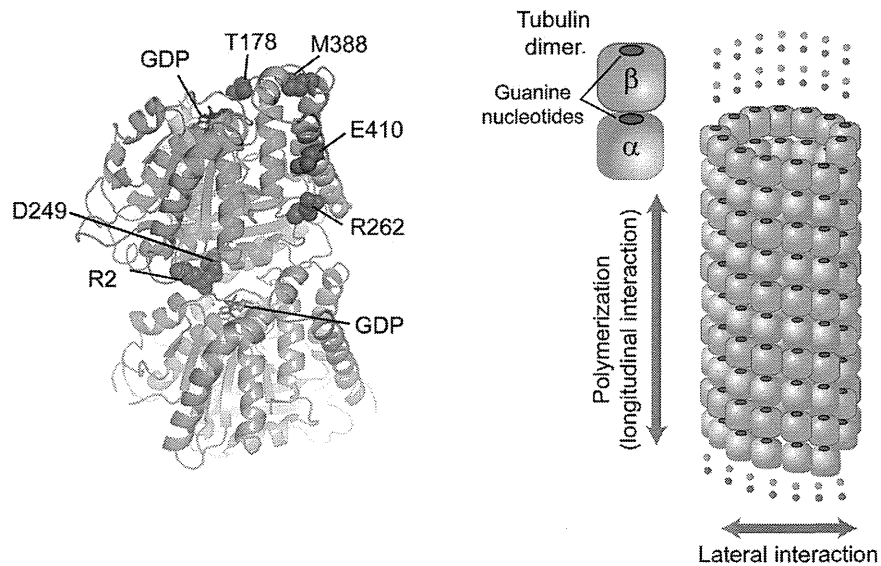
unsteady walking and others never acquiring head control. The maximum motor milestone of these patients was unstable short walking. The clinical course appeared milder in patients with an older age at onset. This tendency was most prominent in patients initially diagnosed with unclassified hypomyelinating leukoencephalopathy. For example, the onset of motor deterioration started in the first or second decades in these patients but was between 0 and 3 years old in patients with typical H-ABC. Intellectual disability was mild to moderate in the former but mostly severe in the latter patients.

All clinically evaluated patients with *TUBB4A* mutations demonstrated cerebellar ataxia and spasticity. Except for patient 8, all demonstrated extrapyramidal features such as rigidity, dystonia, or choreoathetosis. In patient 1, dystonia was prominent compared with other hypomyelination patients with either *POLR3A* or *POLR3B* mutations.^{9,11} Patient 8 was 1 year old at the time of the study, and brain MRI showed a relatively small but still well-retained putamen compared with healthy subjects of the same age, suggesting that extrapyramidal features may not yet have developed but would likely express as the basal ganglia atrophy progressed. Notably, both hypomyelinating patients with either very mild basal ganglia atrophy (patient 2) or none identifiable (patient 1) demonstrated extrapyramidal signs, suggesting that the basal ganglia may be impaired functionally in

these patients as well as other patients with typical H-ABC. Case reports are available in appendix e-1. Patients 1 and 2,⁹ 4,²⁶ and 5²⁷ were previously described. Retrospectively, patient 2 might be diagnosed with atypical H-ABC because minimal basal ganglia atrophy cannot be excluded. In the patient with H-ABC with no *TUBB4A* mutation, the atrophy of basal ganglia was very mild compared with that of patients with typical H-ABC. However, clinical symptoms are very severe with neither head control nor sitting at 12 years, suggesting that the patient has atypical H-ABC.

DISCUSSION The β - and α -tubulins are major components of microtubules. Microtubules have essential roles in many cellular processes including mitosis, intracellular transport, asymmetric neuronal morphology, and ciliary and flagellar motility.²⁸ Multiple β -tubulin isotypes are present, with high homology (differing primarily at 15–20 amino acids within the C terminus), and expressed differentially in a tissue-dependent manner.²⁹ Certain isotypes, namely, β -tubulin isotypes 2A, 2B, 3, and 4A, are neuron-specific proteins and highly expressed in brain.²⁸ In the nervous system, microtubules provide structure, generate force necessary for neuronal migration, and serve as scaffolds for motor proteins and/or MAPs to transport cargo.³⁰ In addition to *TUBB4A*-associated leukoencephalopathies¹⁷ and dystonia,^{18,19} *TUBA1A*, *TUBB2B*, and *TUBB3*

Figure 2 Structural prediction of *TUBB4A* mutations in the $\alpha\beta$ -tubulin heterodimer



Mapping of disease-causing amino acid mutations on the $\alpha\beta$ -tubulin heterodimer (Protein Data Bank code 1JFF) crystal structure, with schematic representation of a tubulin dimer (left) and microtubule segment (right). The α - and β -tubulins are colored gray and green, respectively. Left: The longitudinal interheterodimer interface of β -tubulin (which interacts with α -tubulin in a neighboring $\alpha\beta$ heterodimer) is colored pink,²⁴ and the β -tubulin microtubule-associated protein and motor protein interaction region is colored cyan.^{21,22} Side chains of residues altered by the mutations are shown in space-filling representation in red. Helices, β -sheets, and loops are shown as ribbons, arrows, and threads, respectively, and nucleotides are blue sticks. Right: Tubulin heterodimers polymerize longitudinally to form protofilaments (longitudinal interaction), then laterally interact with each other to form microtubules (lateral interaction). Blue circles represent guanine nucleotide-binding pockets of α - and β -tubulins.

mutations are reported to cause the spectrum of neurologic disorders resulting from neural migration, differentiation, and axon guidance and maintenance abnormalities,²⁵ demonstrating the importance of $\alpha\beta$ -tubulin heterodimers in the nervous system.

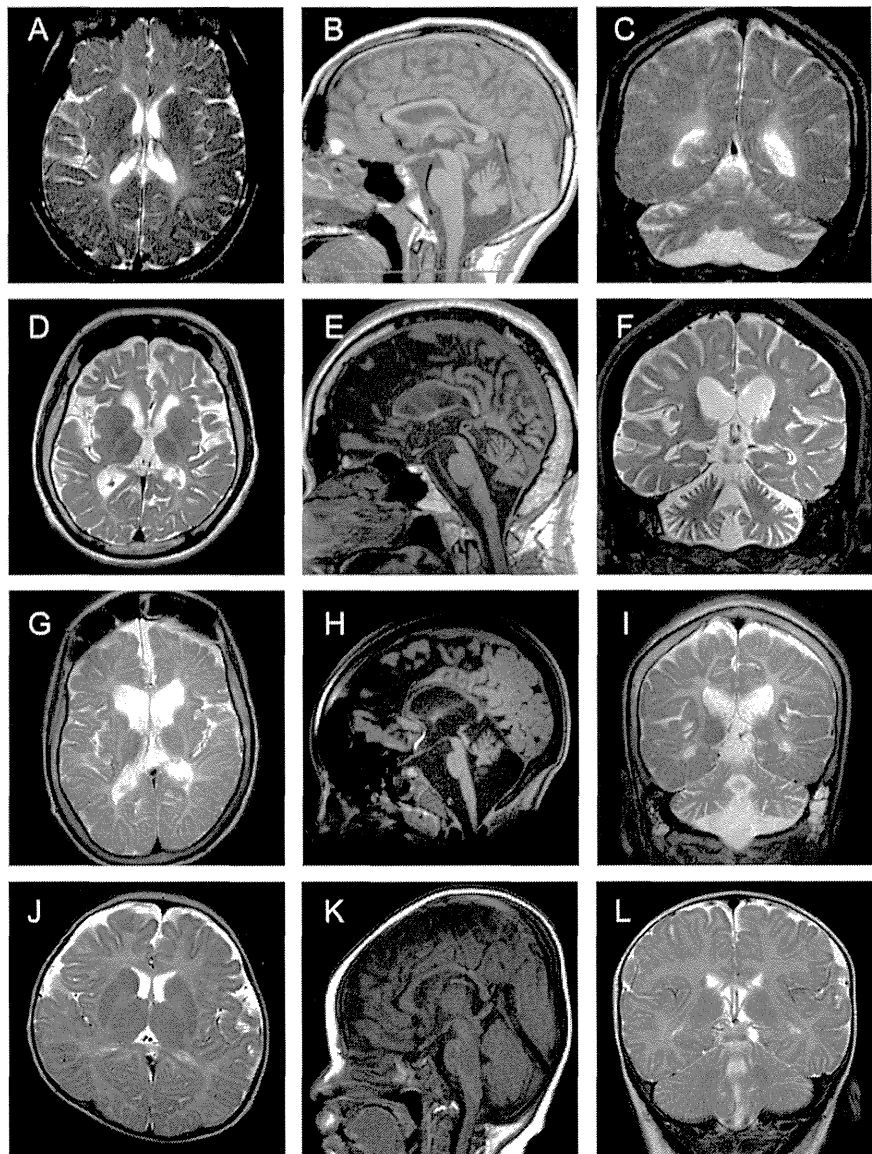
In this study, we identified 6 missense *TUBB4A* mutations, 5 of which are novel, in 6 of 7 patients with H-ABC and 2 of 7 patients initially diagnosed with unclassified hypomyelinating leukoencephalopathy. Of the patients with H-ABC, all 6 patients with *TUBB4A* mutations showed typical H-ABC, supporting that H-ABC is a distinct disease entity caused by *TUBB4A* abnormality. We did not detect any *TUBB4A* mutations in one patient with atypical H-ABC. This may be because this patient has a clinically similar, but different disease, possibly caused by a different mutated gene.

We report a *TUBB4A* mutation in 2 patients with preserved basal ganglia. Their brain MRI findings are similar to patients with *POLR3A* or *POLR3B* mutations, rather than H-ABC. However, it is notable that both patients showed apparent extrapyramidal signs, to suggest functional impairment. Accompanying extrapyramidal features are extremely atypical in patients with either *POLR3A* or *POLR3B* mutations.^{9,11} Furthermore, comparing these 2 patients with other typical H-ABC patients with *TUBB4A* mutations,

patients with minimal basal ganglia atrophy tend to have a milder clinical course. Both patients have a recurrent missense mutation, c.1228G>A (p.Glu410Lys). Based on our 3-dimensional modeling analysis, the Glu410Lys mutation is predicted to directly impair motor protein and/or MAP interactions with microtubules, while the other mutations identified in patients with typical H-ABC may affect longitudinal interactions for maintaining $\alpha\beta$ -tubulin heterodimerization/polymerization. Different effects of the *TUBB4A* mutations on tubulin function may lead to this phenotypic variation. Supporting this hypothesis, the p.Glu410Lys mutation in *TUBB3*, which also directly alters a kinesin motor protein binding site in β -tubulin isotype 3, demonstrates clinically distinct features compared with the other mutations.³⁰ Therefore, the p.Glu410Lys mutation in *TUBB4A* may contribute to the milder end of the phenotypic spectrum of *TUBB4A* mutations. Additional patients with *TUBB4A* mutations are needed to clinically confirm mutational consequences.

Another important finding is that one of the patients with H-ABC had a p.Arg2Gln mutation, since the p.Arg2Gly mutation has recently been identified in patients from a large DYT4 family.^{18,19} DYT4 was described in 1985 in an Australian family that had emigrated from England as whispering dysphonia and generalized dystonia. To date, no other pedigrees

Figure 3 Brain MRI of patients with *TUBB4A* mutations



Axial T2-weighted (A, D, G, J), sagittal T1-weighted (B, E, H, K), and coronal T2-weighted (C, F, I, L) images. Patient 1 at 14 years of age (A); patient 1 at 16 years (B, C); patient 2 at 38 years (D-F); patient 3 at 13 years (G-I); and patient 8 at 7 months of age (J-L). All patients show diffuse cerebral white matter hypomyelination with normal (J), mildly reduced (A), or considerably reduced (D, G) white matter volumes. In patient 1, cerebral white matter hypomyelination is unchanged, comparing at 14 (A) and 16 (B, C) years of age. In patient 1, the putamen and the head of the caudate nucleus are normal in size (A). In patient 2, minimal putamen atrophy cannot be excluded (D). The putamen and the head of the caudate nucleus are small or hardly recognizable in patient 3 (G). In patient 8, the putamen is slightly small compared with a healthy control at the same age (J). The globus pallidus and thalamus are normal in size (A, D, G, J). Atrophy of the cerebellar vermis and hemisphere, and corpus callosum was variably observed in 4 patients, but not patient 8 (B, C, E, F, H, I, K, L).

with this phenotype have been reported worldwide.¹⁸ The symptoms typically emerge in the third decade, following a highly penetrant, autosomal dominant mode of inheritance.³¹ Brain MRI demonstrates normal structural findings. Arg2 resides within the autoregulatory MREI domain of β -tubulin 4A, which is necessary for autoregulation of the β -tubulin messenger RNA transcript. Site-directed mutagenesis shows that any Arg2 substitution leads to loss of

autoregulated instability and increased mutant tubulin subunit levels.³² Thus, mutations in the MREI domain have been assumed to cause DYT4 rather than H-ABC, because of the different impact on *TUBB4A*.¹⁷ However, our study shows that mutations in the MREI domain can also cause the H-ABC phenotype. The phenotypic difference between the p.Arg2Gly and p.Arg2Gln mutations remains unsolved. Because DYT4 is an extremely rare

syndrome that has only been described in one large pedigree so far, patients of the family may have another modifying factor(s) to spare cerebral white matter abnormalities.

Diffuse hypomyelination syndromes are a heterogeneous group of disorders with overlapping clinical features. Currently, they are categorized based on brain MRI findings, which is very useful in clinical practice. Basal ganglia atrophy specifically distinguishes H-ABC from other hypomyelination disorders. Our study shows that *TUBB4A* mutations associate not only with the typical H-ABC cases but also with some hypomyelinating patients with retained basal ganglia, although notably all patients with *TUBB4A* mutations have extrapyramidal features in common. Our study implies that *TUBB4A* may cause hypomyelinating leukoencephalopathies with either a morphologically or a functionally impaired basal ganglia. Extrapyramidal features may be a key for clinicians to examine *TUBB4A* mutations in genetically unsolved hypomyelinating leukoencephalopathies.

AUTHOR CONTRIBUTIONS

Satoko Miyatake: genetic and clinical data analysis, data interpretation, and drafting/revising of the manuscript. Hitoshi Osaka: clinical data analysis and sample collection. Masaaki Shiina: structural data analysis. Masayuki Sasaki, Jun-ichi Takanashi, Kazuhiro Haginoya, Takahiro Wada, Masafumi Morimoto, Naoki Ando, and Yoji Ikuta: clinical data analysis and sample collection. Mitsuko Nakashima, Yoshinori Tsurusaki, and Noriko Miyake: genetic data analysis. Kazuhiro Ogata: structural data analysis. Naomichi Matsumoto: study concept and design, data interpretation, and drafting/revising of the manuscript. Hiroto Saito: study concept and design, genetic data analysis, data interpretation, and drafting/revising of the manuscript.

ACKNOWLEDGMENT

The authors thank all of the participants for their cooperation in this research, and Dr. K. Nishiyama, Ms. K. Takabe, Mr. T. Miyama, Ms. A. Narita, Ms. N. Watanabe, and Ms. S. Sugimoto, from the Department of Human Genetics, Yokohama City University Graduate School of Medicine, for their technical assistance.

STUDY FUNDING

Supported by the Ministry of Health, Labour and Welfare of Japan; the Japan Society for the Promotion of Science (a Grant-in-Aid for Scientific Research [B] [25293085, 25293235]; and a Grant-in-Aid for Scientific Research [A] [13313587]); the Takeda Science Foundation; the fund for Creation of Innovation Centers for Advanced Interdisciplinary Research Areas Program in the Project for Developing Innovation Systems; the Strategic Research Program for Brain Sciences (11105137); and a Grant-in-Aid for Scientific Research on Innovative Areas (Transcription Cycle) from the Ministry of Education, Culture, Sports, Science and Technology of Japan (12024421).

DISCLOSURE

S. Miyatake is funded by research grants from the Yokohama Foundation for Advancement of Medical Science. H. Osaka is funded by research grants from the Ministry of Health, Labour and Welfare of Japan (Research on Rare and Intractable Diseases [H24-Nanchitou-Ippan-072]). M. Shiina and M. Sasaki report no disclosures relevant to the manuscript. J. Takanashi is funded by research grants from the Ministry of Health, Labour and Welfare of Japan (Research on Rare and Intractable Diseases [H24-Nanchitou-Ippan-072]). K. Haginoya, T. Wada, M. Morimoto, N. Ando, Y. Ikuta, M. Nakashima, and Y. Tsurusaki report no disclosures relevant to the

manuscript. N. Miyake is funded by research grants from the Ministry of Health, Labour and Welfare of Japan, a Grant-in-Aid for Scientific Research (B) from the Japan Society for the Promotion of Science, and a research grant from the Takeda Science Foundation. K. Ogata is supported by a Grant-in-Aid for Scientific Research on Innovative Areas (Transcription Cycle) from the Ministry of Education, Culture, Sports, Science and Technology of Japan. N. Matsumoto is supported by grants from the Ministry of Health, Labour and Welfare of Japan, a Grant-in-Aid for Scientific Research (A) from the Japan Society for the Promotion of Science, the Takeda Science Foundation, the fund for Creation of Innovation Centers for Advanced Interdisciplinary Research Areas Program in the Project for Developing Innovation Systems, the Strategic Research Program for Brain Sciences, and a Grant-in-Aid for Scientific Research on Innovative Areas (Transcription Cycle) from the Ministry of Education, Culture, Sports, Science and Technology of Japan. H. Saito is funded by research grants from a Grant-in-Aid for Scientific Research (B) from the Japan Society for the Promotion of Science, and a research grant from the Takeda Science Foundation. Go to Neurology.org for full disclosures.

Received October 10, 2013. Accepted in final form March 20, 2014.

REFERENCES

1. Schiffmann R, van der Knaap MS. Invited article: an MRI-based approach to the diagnosis of white matter disorders. *Neurology* 2009;72:750–759.
2. Steenweg ME, Vanderver A, Blaser S, et al. Magnetic resonance imaging pattern recognition in hypomyelinating disorders. *Brain* 2010;133:2971–2982.
3. Wolf NI, Harting I, Boltshauser E, et al. Leukoencephalopathy with ataxia, hypodontia, and hypomyelination. *Neurology* 2005;64:1461–1464.
4. Timmons M, Tsokos M, Asab MA, et al. Peripheral and central hypomyelination with hypogonadotropic hypogonadism and hypodontia. *Neurology* 2006;67:2066–2069.
5. Vazquez-Lopez M, Ruiz-Martin Y, de Castro-Castro P, Garzo-Fernandez C, Martin-del Valle F, Marquez-de la Plata L. Central hypomyelination, hypogonadotropic hypogonadism and hypodontia: a new leukodystrophy [in Spanish]. *Rev Neurol* 2008;47:204–208.
6. Bernard G, Thiffault I, Tetreault M, et al. Tremor-ataxia with central hypomyelination (TACH) leukodystrophy maps to chromosome 10q22.3-10q23.31. *Neurogenetics* 2010;11:457–464.
7. Atrouni S, Daraze A, Tamraz J, Cassia A, Caillaud C, Megarbane A. Leukodystrophy associated with oligodontia in a large inbred family: fortuitous association or new entity? *Am J Med Genet A* 2003;118A:76–81.
8. Chouery E, Delague V, Jalkh N, et al. A whole-genome scan in a large family with leukodystrophy and oligodontia reveals linkage to 10q22. *Neurogenetics* 2011;12:73–78.
9. Sasaki M, Takanashi J, Tada H, Sakuma H, Furushima W, Sato N. Diffuse cerebral hypomyelination with cerebellar atrophy and hypoplasia of the corpus callosum. *Brain Dev* 2009;31:582–587.
10. Bernard G, Chouery E, Putorti ML, et al. Mutations of POLR3A encoding a catalytic subunit of RNA polymerase Pol III cause a recessive hypomyelinating leukodystrophy. *Am J Hum Genet* 2011;89:415–423.
11. Saito H, Osaka H, Sasaki M, et al. Mutations in POLR3A and POLR3B encoding RNA polymerase III subunits cause an autosomal-recessive hypomyelinating leukoencephalopathy. *Am J Hum Genet* 2011;89:644–651.
12. Tetreault M, Choquet K, Orcesi S, et al. Recessive mutations in POLR3B, encoding the second largest subunit of Pol III, cause a rare hypomyelinating leukodystrophy. *Am J Hum Genet* 2011;89:652–655.

13. Potic A, Brais B, Choquet K, Schiffmann R, Bernard G. 4H syndrome with late-onset growth hormone deficiency caused by POLR3A mutations. *Arch Neurol* 2012;69:920–923.
14. Daoud H, Tetreault M, Gibson W, et al. Mutations in POLR3A and POLR3B are a major cause of hypomyelinating leukodystrophies with or without dental abnormalities and/or hypogonadotropic hypogonadism. *J Med Genet* 2013;50:194–197.
15. van der Knaap MS, Naidu S, Pouwels PJ, et al. New syndrome characterized by hypomyelination with atrophy of the basal ganglia and cerebellum. *AJNR Am J Neuroradiol* 2002;23:1466–1474.
16. van der Knaap MS, Linnankivi T, Paetau A, et al. Hypomyelination with atrophy of the basal ganglia and cerebellum: follow-up and pathology. *Neurology* 2007;69:166–171.
17. Simons C, Wolf NI, McNeil N, et al. A de novo mutation in the beta-tubulin gene TUBB4A results in the leukoencephalopathy hypomyelination with atrophy of the basal ganglia and cerebellum. *Am J Hum Genet* 2013;92:767–773.
18. Hersheson J, Mencacci NE, Davis M, et al. Mutations in the autoregulatory domain of beta-tubulin 4a cause hereditary dystonia. *Ann Neurol* 2013;73:546–553.
19. Lohmann K, Wilcox RA, Winkler S, et al. Whispering dysphonia (DYT4 dystonia) is caused by a mutation in the TUBB4 gene. *Ann Neurol* 2013;73:537–545.
20. Lowe J, Li H, Downing KH, Nogales E. Refined structure of alpha beta-tubulin at 3.5 Å resolution. *J Mol Biol* 2001;313:1045–1057.
21. Uchimura S, Oguchi Y, Katsuki M, et al. Identification of a strong binding site for kinesin on the microtubule using mutant analysis of tubulin. *EMBO J* 2006;25:5932–5941.
22. Al-Bassam J, Ozer RS, Safer D, Halpain S, Milligan RA. MAP2 and tau bind longitudinally along the outer ridges of microtubule protofilaments. *J Cell Biol* 2002;157:1187–1196.
23. Nawrotek A, Knossow M, Gigant B. The determinants that govern microtubule assembly from the atomic structure of GTP-tubulin. *J Mol Biol* 2011;412:35–42.
24. Nogales E, Whittaker M, Milligan RA, Downing KH. High-resolution model of the microtubule. *Cell* 1999;96:79–88.
25. Tischfield MA, Cederquist GY, Gupta ML Jr, Engle EC. Phenotypic spectrum of the tubulin-related disorders and functional implications of disease-causing mutations. *Curr Opin Genet Dev* 2011;21:286–294.
26. Wakusawa K, Haginoya K, Kitamura T, et al. Effective treatment with levodopa and carbidopa for hypomyelination with atrophy of the basal ganglia and cerebellum. *Tohoku J Exp Med* 2006;209:163–167.
27. Hattori A, Ando N, Fujimoto S, Kobayashi S, Ishikawa T, Togari H. A boy with hypomyelination with atrophy of the basal ganglia and cerebellum [in Japanese]. *No To Hattatsu* 2010;42:42–44.
28. Leandro-Garcia LJ, Leskela S, Landa I, et al. Tumoral and tissue-specific expression of the major human beta-tubulin isotypes. *Cytoskeleton* 2010;67:214–223.
29. Sullivan KF, Cleveland DW. Sequence of a highly divergent beta tubulin gene reveals regional heterogeneity in the beta tubulin polypeptide. *J Cell Biol* 1984;99:1754–1760.
30. Chew S, Balasubramanian R, Chan WM, et al. A novel syndrome caused by the E410K amino acid substitution in the neuronal beta-tubulin isotype 3. *Brain* 2013;136:522–535.
31. Parker N. Hereditary whispering dysphonia. *J Neurol Neurosurg Psychiatry* 1985;48:218–224.
32. Yen TJ, Machlin PS, Cleveland DW. Autoregulated instability of beta-tubulin mRNAs by recognition of the nascent amino terminus of beta-tubulin. *Nature* 1988;334:580–585.

Enjoy Big Savings on NEW 2014 AAN Practice Management Webinars Subscriptions

The American Academy of Neurology offers 14 cost-effective Practice Management Webinars you can attend live or listen to recordings posted online. AAN members can purchase one webinar for \$149 or subscribe to the entire series for only \$199. *This is new pricing for 2014 and significantly less than 2013*—and big savings from the new 2014 nonmember price of \$199 per webinar or \$649 for the subscription. Register today for these and other 2014 webinars at AAN.com/view/pmw14:

April 8 – How PQRS Quality Measures Will Inform Future Medicare Value-based Payments

May 13 – Measuring and Improving Your Patients' Experience

June 18 – Using Practice Benchmarking Analytics to Improve Your Bottom Line



Short Report

Genotype–phenotype correlation of contiguous gene deletions of *SLC6A8*, *BCAP31* and *ABCD1*

van de Kamp J.M., Errami A., Howidi M., Anselm I., Winter S., Phalin-Roque J., Osaka H., van Dooren S.J.M., Mancini G.M., Steinberg S.J., Salomons G.S. Genotype–phenotype correlation of contiguous gene deletions of *SLC6A8*, *BCAP31* and *ABCD1*. *Clin Genet* 2015; 87: 141–147. © John Wiley & Sons A/S. Published by John Wiley & Sons Ltd, 2014

The *BCAP31* gene is located between *SLC6A8*, associated with X-linked creatine transporter deficiency, and *ABCD1*, associated with X-linked adrenoleukodystrophy. Recently, loss-of-function mutations in *BCAP31* were reported in association with severe developmental delay, deafness and dystonia. We characterized the break points in eight patients with deletions of *SLC6A8*, *BCAP31* and/or *ABCD1* and studied the genotype–phenotype correlations. The phenotype in patients with contiguous gene deletions involving *BCAP31* overlaps with the phenotype of isolated *BCAP31* deficiency. Only deletions involving both *BCAP31* and *ABCD1* were associated with hepatic cholestasis and death before 1 year, which might be explained by a synergistic effect. Remarkably, a patient with an isolated deletion at the 3'-end of *SLC6A8* had a similar severe phenotype as seen in *BCAP31* deficiency but without deafness. This might be caused by the disturbance of a regulatory element between *SLC6A8* and *BCAP31*.

Conflict of interest

The authors have no conflict of interest.

**J.M. van de Kamp^a, A. Errami^b,
M. Howidi^c, I. Anselm^d,
S. Winter^e, J. Phalin-Roque^e,
H. Osaka^f, S.J.M. van Dooren^g,
G.M. Mancini^h, S.J. Steinbergⁱ
and G.S. Salomons^g**

^aDepartment of Clinical Genetics, VU University Medical Center, Amsterdam, The Netherlands, ^bMRC Holland, Amsterdam, The Netherlands,

^cDepartment of Pediatrics, Mafraq Hospital, Abu Dhabi, UAE, ^dDepartment of Neurology, Boston Children's Hospital, Harvard Medical School, Boston, MA, USA, ^eChildren's Hospital Central California, Madera, CA, USA, ^fClinical Research Institute, Kanagawa Children's Medical Center, Yokohama, Japan,

^gDepartment of Clinical Chemistry, Metabolic Unit, VU University Medical Center, Amsterdam, The Netherlands,

^hDepartment of Clinical Genetics, Erasmus Medical Center, Rotterdam, The Netherlands, and ⁱDepartment of Neurogenetics, Kennedy Krieger Institute & Institute of Genetic Medicine, Johns Hopkins University School of Medicine, Baltimore, MA, USA

Key words: clinical genetics – creatine transporter deficiency – deletion – intellectual disability – liver disease – metabolic disorders – neurology – X-linked adrenoleukodystrophy

Corresponding author: Jiddeke Matuja van de Kamp, Department of Clinical Genetics, VU University Medical Center, [PO BOX 7057] 1007 MB Amsterdam, The Netherlands.

Tel.: +31 20 4440150;

fax: +31 20 4440769;

e-mail: jm.vandekamp@vumc.nl

Received 26 November 2013, revised and accepted for publication 4 February 2014

Loci for the genes *SLC6A8* and *ABCD1* are within a 55-kb span of Xq28. Loss-of-function mutations in *SLC6A8* are associated with X-linked creatine transporter deficiency (CRTR-D), which is characterized by severely reduced brain creatine on ¹H-magnetic resonance spectroscopy (¹H-MRS) and an increased creatine/creatinine ratio in urine. Males present with intellectual disability, severe speech delay, behavioral problems and seizures. The creatine uptake defect can be confirmed in cultured fibroblasts (1).

Loss-of-function mutations in *ABCD1* are associated with X-linked adrenoleukodystrophy (X-ALD), which is characterized by reduced β -oxidation of very long chain fatty acids (VLCFAs), demyelination of white matter and adrenal cortex atrophy. Elevated plasma VLCFA is present at birth. The phenotypic expression of *ABCD1* mutations varies widely. The most severe form, childhood cerebral X-ALD, has an onset usually after 3 years of age; it is characterized by neurological deterioration, often starting with behavioral problems and learning deficits, and later progresses to total disability and death (2).

BCAP31 is located between *SLC6A8* and *ABCD1*. It is in a head-to-head orientation with *ABCD1* and a tail-to-tail orientation with *SLC6A8*. In 2002, Corzo et al. (3) reported three male newborns with large *ABCD1* deletions that extended into *BCAP31* (*DXS1357E*). They had profound hypotonia, developmental delay, hepatic cholestasis and death prior to their first birthday. This severe neonatal presentation has never been observed in isolated *ABCD1* defects. The extent of the contiguous gene deletions was not determined in all the three boys, but the patient with the smallest deletion was characterized and showed that the critical region included the 5' coding exons of *BCAP31* and *ABCD1*. The syndrome was named 'contiguous *ABCD1* *DXS1357E* deletion syndrome' (CADDs). A fourth CADDs patient with a similar phenotype has been reported; he had a large deletion spanning seven genes: *BCAP31*, *ABCD1*, *PLXNB3*, *SRPK3*, *IDH3G*, *SSR4* and *PDZD4* (4).

Large deletions involving *SLC6A8* were reported in three boys with a more severe presentation than in classic CRTR-D; they had pronounced hypotonia and developmental delay, severe failure to thrive and dystonia or choreathetoid movements (5, 6). In one patient, the deletion extended into *BCAP31* (6). However, the deletion size was not determined in the other two patients (5).

These studies suggest that the clinical phenotypes associated with *ABCD1* or *SLC6A8* deficiencies were exacerbated by concomitant knockout of *BCAP31*. Just recently, isolated loss-of-function mutations in *BCAP31* were reported in association with a severe phenotype combining deafness, dystonia and cerebral hypomyelination (DDCH, MIM 300475) (7). Conclusions regarding the contribution of the separate genes in contiguous gene deletions involving *SLC6A8*, *BCAP31* and/or *ABCD1* were hampered by the fact that the deletion size was not determined in all the seven reported patients (3, 5). We characterized the break

points in five patients and provide an update of the patients who were alive at the time of the previous report (5, 6). In addition, we describe two new patients with a CADDs and one patient with an isolated partial *SLC6A8* deletion. We discuss the genotype–phenotype correlations in all the 10 patients.

Materials and methods

Materials and patients

DNA was isolated from blood or cultured fibroblasts of eight patients with suspected large gene deletions of *SLC6A8* and/or *ABCD1*. Three patients were suspected of *SLC6A8* deletions and five patients of *ABCD1* deletions, based on clinical and biochemical features and the absence of polymerase chain reaction (PCR) products of the involved gene. Case reports of two patients with *SLC6A8* deletions (5, 8) and three patients with CADDs (3) were previously reported. In addition, the genotype and phenotype of two previously reported contiguous gene deletion patients (4, 6) were reviewed (patients 9 and 10).

Break point analysis

Multiplex ligation-dependent probe amplification (MLPA) using the P049 kit with probes for several exons of *SLC6A8*, *BCAP31*, *ABCD1* and neighboring genes was performed to confirm the deletions and to estimate their size. To narrow down the regions of the break point, PCRs of about 200 bp in intervals of ~5–10 kb were designed flanking the deleted MLPA probes. Finally, long-range PCR over the break point was performed followed by DNA sequencing to reveal the exact break points. All primers were designed with a high specificity for the X-chromosome, as a paralogous gene region occurs on chromosome 16.

RNA analysis of *BCAP31*

RNA was isolated from the available fibroblasts of patients 2–6 and 9. Subsequently, cDNA was synthesized using oligodT. In order to study whether the deletions resulted in truncated transcripts, we amplified specific regions of the *BCAP31* transcript (i.e. exons 1–8, 1–4 and 5–8) using specific reverse transcription polymerase chain reaction (RT-PCR) primers.

Results

Break point analysis

The break points were sequenced by long-range PCR in seven patients (Appendix S1, Supporting information). Although long-range PCR was unsuccessful in eighth patient (patient 6), MLPA and locus-specific PCR analyses narrowed down the break point sites to between exons 5 and 8 in *BCAP31* and between exons 7 and 8 in *ABCD1*. In total, of the 10 patients reported here, 2 had isolated partial *SLC6A8* deletions and 8

Gene deletions of *SLC6A8*, *BCAP31* and *ABCD1*

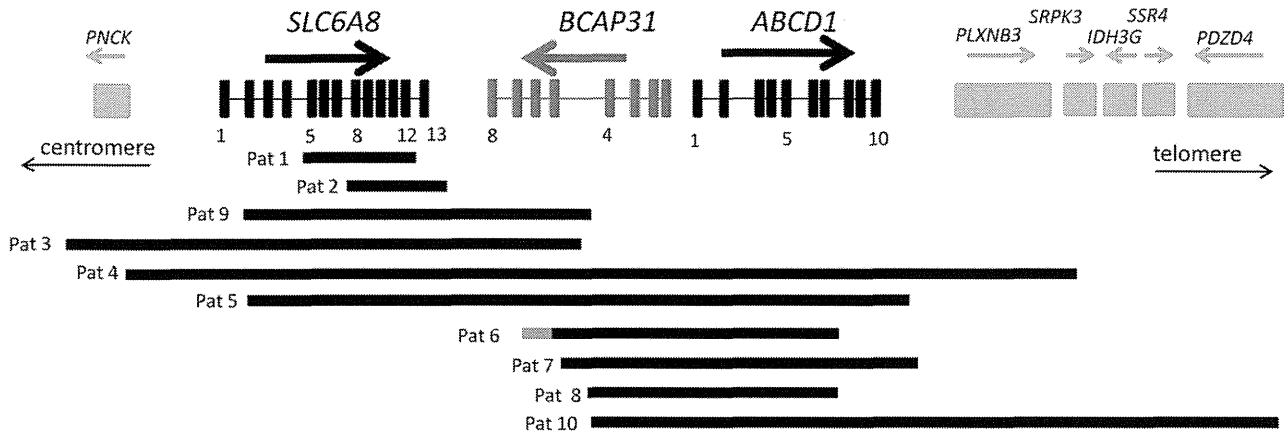


Fig. 1. Location and size of the deletions on Xq28. Deletions are depicted with black bars. The exact break point in patient 6 is unknown and the uncertainty of the involvement of *BCAP31* exons 6 and 7 in the deletion is depicted by a gray bar.

had a contiguous gene deletion involving *BCAP31* and *SLC6A8* and/or *ABCD1* (Fig. 1; Table 1).

Genotype–phenotype correlation

The clinical features of the patients are summarized in Table 1. The patients with contiguous gene deletions involving *BCAP31* ($n=8$) shared many features: profound developmental delay, severe failure to thrive, sensorineural hearing loss and childhood death. Seizures occurred in some. All the patients with deletions involving both *BCAP31* and *ABCD1* ($n=6$) developed cholestatic liver disease and died in the first year of life. It is not documented whether the cause of death was related to liver failure in all cases. By contrast, patients with deletions of *SLC6A8* and *BCAP31* but not *ABCD1* ($n=2$) did not develop cholestatic liver disease, survived until at least 6 years and developed severe dystonia and choreoathetosis after 3 years. Patient 2 with an isolated deletion of exons 8–13 of *SLC6A8* also had a severe presentation with death at 8 years, but without sensorineural hearing loss. By contrast, patient 1 with an isolated deletion of exons 5–12 of *SLC6A8* had a phenotype consistent with classic CRTR-D.

RNA analysis of *BCAP31*

RT-PCR confirmed the absence of *BCAP31* transcripts in patients 4–6. A truncated transcript of exons 1–4 was present in patients 3 and 9. In patient 2, a full-length *BCAP31* transcript was detected (Appendix S1, Supporting information). Because patient 2 had a severe phenotype that suggested *BCAP31* deficiency, the open reading frame and splice sites of *BCAP31* gDNA were additionally sequenced; no pathogenic mutation was identified.

Discussion

The phenotype of patients with contiguous gene deletions involving *BCAP31* was more severe, overall,

than the isolated defects of *SLC6A8* (causing CRTR-D) or *ABCD1* (causing X-ALD); this suggests an important role for *BCAP31* in patients harboring these contiguous gene deletions. *BCAP31* encodes B-cell-receptor-associated protein 31 (BAP31), an integral membrane protein that is localized in the endoplasmic reticulum (ER) membrane (9). It is a protein-sorting factor that controls the fates (egress, retention, survival and degradation) of newly synthesized integral membrane proteins (10). However, BAP31 is also involved in apoptosis, participating in ER–mitochondrial apoptosis signaling. The mitochondrial fission protein Fission 1 (Fis1) interacts with BAP31 at the ER, forming a platform for recruitment and activation of procaspase-8 during Fas-mediated apoptosis (11). BAP31 is cleaved by caspase-8, generating p20 that remains integrated in the membrane (9, 12). p20 induces apoptosis (9) by causing a rapid transfer of ER calcium into the mitochondria, which leads to mitochondrial recruitment of dynamin-like protein 1 (Dlp1) and mitochondrial fission (12). By contrast, full-length BAP31 inhibits Fas-mediated apoptosis (13). BAP31 also associates with the components of the cytoskeleton actomyosin complex, suggesting that BAP31 may play a role in the structural organization of the cytoplasm (14).

Recently, loss-of-function mutations in *BCAP31* were found in seven individuals from three families presenting with severe motor and intellectual disability, dystonia, sensorineural deafness, hypomyelination, failure to thrive and early death. Fibroblasts of affected individuals showed altered ER morphology and disorganized Golgi; however, contrary to expectation, there was not an excessive accumulation of unfolded proteins or exacerbated cell death (7). The profound developmental delay, sensorineural hearing loss, failure to thrive and childhood death in the patients with contiguous gene deletions involving *BCAP31* are very similar to the isolated *BCAP31* defects and confirm the association of loss of *BCAP31* with this phenotype.

Neonatal hepatic cholestasis leading to liver failure and death in the first year was restricted to the patients with deletions involving both *ABCD1* and *BCAP31* and

Table 1. Clinical features. Patient order is based on the location of the deletion (from centromeric to telomeric)

Patient	1	2	9	3	4	5	6	7	8	10	CRTR-D	BCAP31	X-ALD
Deletion size	2.1 kb	4.9 kb	19 kb	40 kb	110 kb	64 kb	34–42 kb	50 kb	31 kb	90 kb	Isolated defect	Isolated defect	Isolated defect
Involved genes	<i>SLC6A8</i>	<i>SLC6A8</i>	<i>SLC6A8</i> , <i>BCAP31</i>	<i>PNCK</i> , <i>SLC6A8</i> , <i>BCAP31</i>	<i>PNCK</i> , <i>SLC6A8</i> , <i>BCAP31</i> , <i>ABCD1</i> , <i>PLXNB3</i> , <i>SRPK3</i>	<i>SLC6A8</i> , <i>BCAP31</i> , <i>ABCD1</i>	<i>BCAP31</i> , <i>ABCD1</i>	<i>BCAP31</i> , <i>ABCD1</i>	<i>BCAP31</i> , <i>ABCD1</i>	<i>BCAP31</i> , <i>ABCD1</i> , <i>PLXNB3</i> , <i>SRPK3</i> , <i>IDH3G</i> , <i>SSR4</i> , <i>PDZD4</i>	<i>SLC6A8</i>	<i>BCAP31</i>	<i>ABCD1</i>
Age	40 years	Died 8 years, septic shock	9 years	Died 8 years, unknown cause	Died <5 months	Died 4 months, LF, RF	Died 8 months	Died 11 months, LF, GI bleeding	Died 4 months, RF, GI bleeding	Died 8 months, pneumonia, sepsis	Normal life expectancy	Death, 7 months –24 years ^a	Average death at 9.4 years
Development	Walking at 2 years, speaks single words	Smiles, eye contact, no milestones attained	Profound delay, no head control	Some eye contact, no milestones attained	?	Profound delay	Delayed, smiles, alert and active at 4 mo, sedated at 7 months	Profound delay	Profound delay	No milestones attained	Mild-severe delay, walking at mean age of 2 years	No milestones attained or only head control ^a	Early develop- ment normal, onset neurological deterioration usually >3 years
Motor symptoms	–	Profound axial hypotonia, hypertonic limbs, quadriplegia	Hypertonic	Profound neonatal hypotonia	Hypertonic	Profound neonatal hypotonia	Hypotonia	Profound neonatal hypotonia	Profound neonatal hypotonia	Hypotonia	Mild hypotonia	Pyramidal signs, quadriplegia	Neurological deterioration >3 years
Extrapyramidal	–	Dystonia from 3 months; severe choreoa- thetosis from 4–5 years	Severe dystonia and athetosis from 4 months	Severe choreoa- thetosis from 3 years	?	–	–	Frequent episodes of opistho- tonus, bruxism	–	–	Mild choreoa- thetosis or dystonia in some patients	Severe dystonia	–
Seizures (onset)	2 years	–	4 years status	4 years	?	2 months	–	–	2 months	–	+/-	+/-	+/-
FTT (height and weight)	–	–3 to –4 SD	–3 to –4 SD	–3 SD	?	++, IUGR	–3 to –4 SD	++	++	–6 SD, IUGR	+/-	–2 to –8 SD, IUGR	–
Head circumference	0 SD	–3 SD	?	–2.5 SD	?	?	–3 SD	?	?	–10 SD	Normal	–2 to –5 SD	Normal
Hepatic	–	–	Mildly elevated liver transami- nases	Transient elevated liver transami- nases	Cholestasis	Cholestasis	Cholestasis	Cholestasis	Cholestasis	Cholestasis	–	Transient elevated liver transami- nases	–
Congenital SNHL	– ^b	– ^c	+	+	+	?	?	+	+	+	–	+	–
Ophthalmological	–	Strabismus	Does not pursue objects	Pigmentary retinopathy at 3 years	?	?	–	Cataract	?	Blind	Strabismus	Strabismus, optic atrophy	–
Dysmorphic	Mild	–	–	+ ^d	?	–	Mild ^d	–	–	+ ^d	Mild atypical	+/-	–